J|A|C|S
ARTICLES
Published on Web 06/09/2005

Reexamination of Lead(II) Coordination Preferences in Sulfur-Rich Sites: Implications for a Critical Mechanism of Lead Poisoning

John S. Magyar,[†,○] Tsu-Chien Weng,[§,#] Charlotte M. Stern,[†] David F. Dye,[||] Brian W. Rous,[†] John C. Payne,[†] Brian M. Bridgewater,[⊥,▽] Ana Mijovilovich,[§] Gerard Parkin,[⊥] Jeffrey M. Zaleski,[||] James E. Penner-Hahn,*[,§] and Hilary Arnold Godwin*[,†,‡]

Contribution from the Department of Chemistry, Northwestern University, 2145 Sheridan Road, Evanston, Illinois 60208-3113, Department of Biochemistry, Molecular Biology, and Cell Biology, Northwestern University, 2153 North Campus Drive, Evanston, Illinois 60208-3300, Department of Chemistry, University of Michigan, 930 North University, Ann Arbor, Michigan 48109-1055, Department of Chemistry, Indiana University, 800 East Kirkwood Avenue, Bloomington, Indiana 47405-7102, and Department of Chemistry, Columbia University, New York, New York 10027

Received December 15, 2004; Revised Manuscript Received April 29, 2005; E-mail: h-godwin@northwestern.edu; jeph@umich.edu

Abstract: Recent studies suggest that the developmental toxicity associated with childhood lead poisoning may be attributable to interactions of Pb(II) with proteins containing thiol-rich structural zinc-binding sites. Here, we report detailed structural studies of Pb(II) in such sites, providing critical insights into the mechanism by which lead alters the activity of these proteins. X-ray absorption spectroscopy of Pb(II) bound to structural zinc-binding peptides reveals that Pb(II) binds in a three-coordinate Pb(II)-S_3 mode, while Zn(II) is known to bind in a four-coordinate mode in these proteins. This Pb(II)-S_3 coordination in peptides is consistent with a trigonal pyramidal Pb(II)-S_3 model compound previously reported by Bridgewater and Parkin, but it differs from many other reports in the small molecule literature which have suggested Pb(II)-S_4 as a preferred coordination mode for lead. Reexamination of the published structures of these "Pb(II)-S_4" compounds reveals that, in almost all cases, the coordination number of Pb is actually 5, 6, or 8. The results reported herein combined with this new review of published structures suggest that lead prefers to avoid four-coordination in sulfur-rich sites, binding instead as trigonal pyramidal Pb(II)-S_3 or as Pb(II)-S_{5-8}. In the case of structural zinc-binding protein sites, the observation that lead binds in a three-coordinate mode, and in a geometry that is fundamentally different from the natural coordination of zinc in these sites, explains why lead disrupts the structure of these peptides and thus provides the first detailed molecular understanding of the developmental toxicity of lead.

Introduction

Lead poisoning remains one of the most prevalent diseases of environmental origin in the United States today, particularly affecting young children. The U.S. Centers for Disease Control and Prevention (CDC) currently estimates that 2.2% of all U.S. children aged 1−5 years (434,000 children) have elevated blood lead levels (BLLs) (i.e., ≥10 μg/dL).[1,2] The percentage of children affected is significantly higher than this average in some communities; in the city of Chicago in 2003, ca. 6% of children aged 1−6 years had BLLs ≥ 10 μg/dL, with the percentage of affected children >15% in several neighborhoods.[3] Although the symptoms and effects of lead poisoning are well documented, the detailed molecular mechanisms of lead toxicity remain unknown. Since the range of symptoms associated with lead poisoning is so broad, it is likely that lead affects several different types of proteins and that there are multiple mechanisms of lead toxicity.[4]

One of the best documented targets for lead is the second enzyme in the heme biosynthetic pathway, a zinc enzyme alternately called aminolevulinic acid dehydratase (ALAD) or porphobilinogen synthase (PBS).[4,5] Inhibition of ALAD by lead

[†] Department of Chemistry, Northwestern University.
[‡] Department of Biochemistry, Molecular Biology, and Cell Biology, Northwestern University.
[§] University of Michigan.
[||] Indiana University.
[⊥] Columbia University.
[○] Current address: Beckman Institute, California Institute of Technology, Pasadena, CA 91125.
[#] Current address: Advanced Photon Source, Argonne National Laboratory, Argonne, IL 60439.
[▽] Current address: Rohm and Haas Company, Springhouse, PA.

(1) Centers for Disease Control and Prevention. Children's Blood Lead Levels in the United States. http://www.cdc.gov/nceh/lead/research/kidsBLL.htm (accessed November 2004).
(2) Centers for Disease Control and Prevention *Morbidity and Mortality Weekly Report* **2000**, *49*, 1133−1137.
(3) Chicago Department of Public Health. 2003 Blood Lead Testing Data. http://www.ci.chi.il.us/health/Lead/CAData.html (accessed November, 2004).
(4) Godwin, H. A. *Curr. Opin. Chem. Biol.* **2001**, *5*, 223−227.
(5) Warren, M. J.; Cooper, J. B.; Wood, S. P.; Shoolingin-Jordan, P. M. *Trends Biochem. Sci.* **1998**, *23*, 217−221.

is likely to be a major contributor to the lead-poisoning-associated anemia observed in individuals with high blood lead levels (BLLs $\geq$ 40 μg/dL).[5] ALAD is inhibited by femtomolar concentrations of lead in vitro,[6] and activity of ALAD in vivo inversely correlates with blood lead level.[7] The crystal structure of this enzyme reveals that ALAD contains an unusual Zn(II)-Cys_3 (i.e., Zn(II)-S_3) active site and that Pb(II) binds to this site in a trigonal pyramidal geometry.[5,8−10] Studies by Bridgewater and Parkin on a scorpionate Pb(II)-S_3 model compound reveal that Pb(II) has a 500-fold greater affinity for trigonal S_3 sites than does Zn(II), explaining why lead is such a potent inhibitor of this form of ALAD.[11]

However, inhibition of ALAD by Pb(II) does not account for the developmental and behavioral problems seen in children with very low levels of lead (BLLs $\geq$ 5 μg/dL),[12] and identifying molecular targets that could account for these effects remains a high priority for the pediatric health-care community. Recent work by Godwin and co-workers suggests that transcription factors that contain cysteine-rich (Cys_4) structural zinc-binding sites are promising targets for Pb(II).[13,14] By contrast, other groups have suggested that Pb(II) may target traditional Cys_2-His_2 "zinc-finger" proteins.[15−20] Studies by Godwin and co-workers on a series of model peptides reveal that Pb(II) binds most tightly, and with higher affinity than Zn(II), to the peptide with a Cys_4 site, and lead cannot compete effectively with zinc for binding to the Cys_2His_2 site.[13] This result is particularly significant because proteins containing Cys_4 sites (e.g., steroid receptors and GATA proteins) play critical roles in regulating many developmental processes affected by lead poisoning, such as neurological development and red blood cell formation.[4,14,21−27] In these proteins, tetrahedral coordination of Zn(II) is absolutely required for correct protein folding and for nucleic acid binding activity.[28] Previous work by Godwin and co-workers has shown that even though Pb(II) binds very tightly (log $K_b \geq 12$) to cysteine-rich structural zinc-binding sites, Pb(II) does not stabilize the properly folded form of the protein, as shown by 1D and 2D DQ-COSY ^{1}H NMR and by circular dichroism spectroscopy.[13] In this way, lead binding may have severe implications for developmental processes controlled by these transcription factors. However, the *reason* that Pb(II) does not promote proper protein folding has remained a mystery.

Here, we report detailed structural studies on the coordination geometry of four Pb(II)-peptide complexes and two Pb(II) coordination compounds. We have used X-ray absorption spectroscopy (XAS) to characterize the lead-bound forms of a series of structural zinc-binding peptides as well as the tris(2-mercapto-1-phenylimidazolyl)hydroborato lead complex [(Tm^{Ph})-Pb][ClO_4] (**1**) and tetraphenylarsonium Pb(II) *iso*-maleonitriledithiolate, $[AsPh_4]_4[Pb_2(i\text{-mnt})_4]$ (**2**).[11,29,30] In addition, we

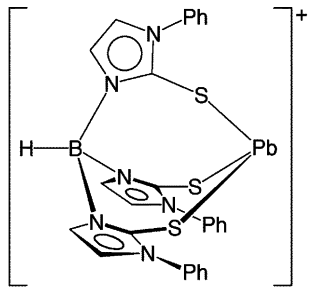

1

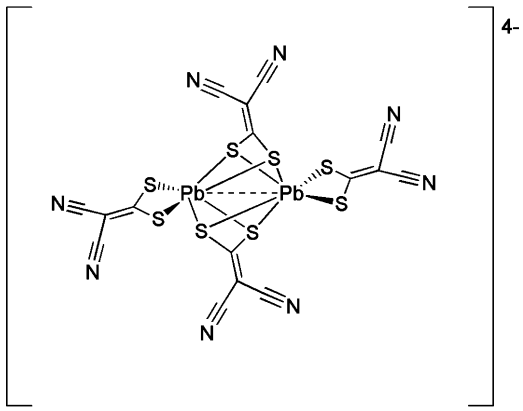

2a

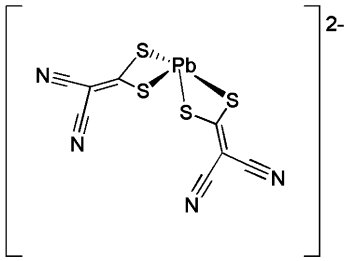

2b

report the low-temperature UV−visible absorption spectra of the series of Pb−peptide complexes and the affinity of Pb(II)

(6) Simons, T. J. B. *Eur. J. Biochem.* **1995**, *234*, 178−183.
(7) Millar, J. A.; Battistini, V.; Cumming, R. L.; Carswell, F.; Goldberg, A. *Lancet* **1970**, *2*, 695−698.
(8) Erskine, P. T.; Norton, E.; Cooper, J. B.; Lambert, R.; Coker, A.; Lewis, G.; Spencer, P.; Sarwar, M.; Wood, S. P.; Warren, M. J.; Shoolingin-Jordan, P. M. *Biochemistry* **1999**, *38*, 4266−4276.
(9) Erskine, P. T.; Senior, N.; Awan, S.; Lambert, R.; Lewis, G.; Tickle, I. J.; Sarwar, M.; Spencer, P.; Thomas, P.; Warren, M. J.; Shoolingin-Jordan, P. M.; Wood, S. P.; Cooper, J. B. *Nat. Struct. Biol.* **1997**, *4*, 1025−1031.
(10) Jaffe, E. K.; Martins, J.; Li, J.; Kervinen, J.; Dunbrack, R. L., Jr. *J. Biol. Chem.* **2001**, *276*, 1531−1537.
(11) Bridgewater, B. M.; Parkin, G. *J. Am. Chem. Soc.* **2000**, *122*, 7140−7141.
(12) Lanphear, B. P.; Dietrich, K.; Auinger, P.; Cox, C. *Public Health Reports* **2000**, *115*, 521−529.
(13) Payne, J. C.; ter Horst, M. A.; Godwin, H. A. *J. Am. Chem. Soc.* **1999**, *121*, 6850−6855.
(14) Ghering, A. B.; Miller Jenkins, L. M.; Schenck, B. L.; Deo, S.; Mayer, R. A.; Pikaart, M. J.; Omichinski, J. G.; Godwin, H. A. *J. Am. Chem. Soc.* **2005**, *127*, 3751−3759.
(15) Zawia, N. H.; Sharan, R.; Brydie, M.; Oyama, T.; Crumpton, T. *Dev. Brain Res.* **1999**, *107*, 291−298.
(16) Zawia, N. H.; Crumpton, T.; Brydie, M.; Reddy, G. R.; Razmiafshari, M. *NeuroToxicology* **2000**, *21*, 1069−1080.
(17) Razmiafshari, M.; Zawia, N. H. *Toxicol. Appl. Pharmacol.* **2000**, *166*, 1−12.
(18) Razmiafshari, M.; Kao, J.; d'Avignon, A.; Zawia, N. H. *Toxicol. Appl. Pharmacol.* **2001**, *172*, 1−10.
(19) Crumpton, T.; Atkins, D. S.; Zawia, N. H.; Barone, S., Jr. *NeuroToxicology* **2001**, *22*, 49−62.
(20) Hanas, J. S.; Rodgers, J. S.; Bantle, J. A.; Cheng, Y. G. *Mol. Pharmacol.* **1999**, *56*, 982−988.
(21) Mangelsdorf, D. J.; Thummel, C.; Beato, M.; Herrlich, P.; Schutz, G.; Umesono, K.; Blumberg, B.; Kastner, P.; Mark, M.; Chambon, P.; Evans, R. M. *Cell* **1995**, *83*, 835−839.
(22) Katzenellenbogen, J. A.; Katzenellenbogen, B. S. *Chem. Biol.* **1996**, *3*, 529−536.
(23) Schwabe, J. W. R.; Rhodes, D. *Trends Biochem. Sci.* **1991**, *16*, 291−296.
(24) Ghering, A. B.; Shokes, J. E.; Scott, R. A.; Omichinski, J. G.; Godwin, H. A. *Biochemistry* **2004**, *43*, 8346−8355.
(25) Tsai, F. Y.; Keller, G.; Kuo, F. C.; Weiss, M.; Chen, J.; Rosenblatt, M.; Alt, F. W.; Orkin, S. H. *Nature* **1994**, *371*, 221−226.
(26) Patient, R. K.; McGhee, J. D. *Curr. Opin. Genet. Dev.* **2002**, *12*, 416−422.
(27) Cantor, A. B.; Orkin, S. H. *Oncogene* **2002**, *21*, 3368−3376.
(28) Berg, J. M.; Godwin, H. A. *Annu. Rev. Biophys. Biomol. Struct.* **1997**, *26*, 357−371.
(29) Hummel, H.-U.; Meske, H. *Z. Naturforsch.* **1989**, *44b*, 293−295.
(30) Hummel, H.-U.; Meske, H. *J. Chem. Soc., Dalton Trans.* **1989**, 627−630.

binding to these domains. These studies reveal significant differences between the Pb(II) coordination geometry and that of Zn(II) in the same peptides, and we propose that the difference in coordination preference and geometry is a concrete way that lead binding disrupts the structure and function of these domains and thus contributes to the developmental problems associated with lead poisoning.

Experimental Section

Sample Preparation. Synthetic peptides[31−34] from Bio-Synthesis, Inc. (Lewisville, TX) were reduced with 10 equiv of dithiothreitol per cysteine, purified to homogeneity by C_{18} reversed-phase HPLC, and handled anaerobically as described previously.[13,35] The total peptide concentration is determined by A_{280} (ϵ_{280} = 1400 M^{-1} cm^{-1}); the concentration of reduced peptide is determined by analysis with 5,5′-dithiobis(2-nitrobenzoic acid) (DTNB).[13,36]

Peptide solutions for low-temperature UV−visible absorption spectroscopy (LT UV−vis) or for XAS were prepared in 100 mM bis(2-hydroxyethyl)amino-tris(hydroxymethyl)methane (Bis-Tris, SigmaUltra grade; Sigma, St. Louis, MO), buffered with boric acid (Sigma) to pH 7.2. Peptides were metalated with 0.9 equiv of Pb(II) [as $Pb(NO_3)_2$, atomic absorption standard solution; Aldrich, Milwaukee, WI]; 30−40% v/v glycerol was added as a glassing agent. Peptide concentrations for LT UV−vis were ca. 0.4 mM; an aliquot of this sample was removed and diluted to ca. 20 μM for the measurement of the room-temperature absorption spectrum. The absorption spectrum without glycerol present was also recorded; spectra were collected using either an HP 8453 or a PerkinElmer Lambda 800 UV−vis spectrophotometer. Samples were prepared at Northwestern, frozen in liquid nitrogen, and shipped overnight on dry ice to the University of Indiana. Peptide samples for XAS (ca. 1 mM) were prepared in the same way as those for LT UV−vis, loaded into Lucite XAS cells with polypropylene windows (total volume ca. 120 μL), frozen in liquid nitrogen, and sent overnight on dry ice to the synchrotron (Stanford Synchrotron Radiation Laboratory, SSRL). At SSRL, the frozen samples were transferred to liquid nitrogen for storage and were kept frozen until data collection.[37] Room-temperature UV−vis absorption spectra of peptide samples both with and without glycerol present were collected using an HP 8453 spectrophotometer.

The Pb(II) model compounds **1** and **2** were synthesized as described in the literature.[11,29,30]

Metal-Binding Titration of CP−CCCH. The Pb−peptide binding constant for CP−CCCH was determined by the same methods used previously for the other consensus peptides.[13] Since K_b^{Co} and K_b^{Zn} were also unknown for CP−CCCH, these binding constants were also determined by literature methods.[35,38] Cobalt was titrated into a mixture of CP−CCHH and CP−CCCH to determine K_b^{Co}; K_b^{Zn} was then determined by competition by titrating a solution of Co−CP−CCCH with Zn(II).[35,38] Once K_b^{Zn} is known, then K_b^{Pb} can be determined through Pb(II)/Zn(II) competition titrations.[13] Data were analyzed using SPECFIT/32,[39] which allows known spectra and binding constants to be input for a large number of species and for the fit to be performed over the entire spectral region of interest. Representative titration data and fits are available in the Supporting Information (Figures S5, S6).

Low-Temperature Absorption Spectroscopy. Low-temperature electronic spectra were recorded using a PerkinElmer Lambda 19 UV−vis−NIR absorption spectrometer with an Oxford Instruments OptistatBath liquid helium optical dewar placed in the sample compartment. Samples were prepared in an inert atmosphere wetbox and were injected into a 150 μL copper cell with two quartz windows separated by a 3 mm permeable synthetic rubber spacer. Samples were frozen in liquid nitrogen before removal from the wetbox and were kept frozen during loading into the cryostat. Spectra were collected at 1.8−4 K using a scan rate of 120 nm min^{-1} and a 2 nm band-pass.

XAS Data Collection and Analysis. XAS data for the Pb L_{III} edge were collected at SSRL beam line 9−3 using a Si(220) double crystal monochromator with a focusing mirror for harmonic rejection. The beam energy was 3 GeV, and the beam size was 1 × 4 mm^2. The X-ray energies were calibrated by collecting the absorption spectrum of a Pb foil reference at the same time as the fluorescence data, with the first inflection point of the L_{III} edge of the Pb foil assigned as 13 038.0 eV. The sample temperature was maintained at 10−12 K during data collection using an Oxford liquid helium flow cryostat. XAS data were collected as fluorescence excitation spectra using a 30-element Ge solid-state detector array. Spectra were measured in 5 eV increments in the pre-edge region (12 810−13 015 eV), 0.5 eV increments in the edge region (13 020−13 070 eV), and 0.05 $Å^{-1}$ increments in the EXAFS region (2.75−13.2 $Å^{-1}$), with an integration time of 1 s in the pre-edge and edge and 1−20 s (k^3 weighted) in the EXAFS region, for a total scan time of 30 min. For all samples, the first and last spectra were compared to confirm the lack of radiation damage during the measurements.

Each channel of each scan was examined for monochromator glitches. The fluorescence from the good channels was averaged for each sample to give the raw data. EXAFS data were extracted using a three-region cubic spline above the edge, followed by normalization to a Victoreen polynomial. Data were converted to k space, $k = [2m_e(E - E_0)/h^2]$, using a threshold energy (E_0 = 13 034.8 eV) that was calibrated by fitting the EXAFS data for the crystallographically characterized reference compound tetraphenyllead, $Pb(C_6H_5)_4$.

Data analysis utilized the EXAFSPAK program suite.[40] The EXAFS data, $\chi(k)$, were fit to the equation

$$\chi(k) = \sum_s \frac{N_s A_{as}(k)}{kR_{as}^2} \exp(-2\sigma_{as}^2 k^2) \sin[2kR_{as}(k) + \phi_{as}(k)]$$

where N_s is the number of scatterers with atom type s at a distance of R_{as}, $A_{as}(k)$ is the effective backscattering amplitude function, σ_{as}^2 is the Debye−Waller factor (disorder in R_{as}), and $\phi_{as}(k)$ is the phase shift of the photoelectron wave traveling between the potentials of the absorbing and scattering atoms. The amplitude and phase functions, $A_{as}(k)$ and $\phi_{as}(k)$, were calculated using *FEFF* 7.02,[41,42] with an amplitude scale factor (0.9) and the threshold energy E_0 calibrated by fitting crystallographically defined model complexes. Raw data were k^3-weighted, and the individual fits were performed in k space (2.0^{-1}3.0 $Å^{-1}$), allowing R_{as} and σ_{as}^2 to vary for each shell, while N_s was held fixed at reasonable integer values.[37]

XANES Simulations. XANES spectra were simulated using *FEFF* 8.2, with muffin tin potentials overlapped by 15%, using the Hedin−

(31) The sequence for the zinc finger consensus peptide that has four cysteines in the zinc-binding site (CP−CCCC) is: PYKCPECGKSFSQKSDLVKCQRTCTG.
(32) The sequence for the zinc finger consensus peptide that has three cysteines followed by a histidine in the zinc-binding site (CP−CCCH) is: PYKCPECGKSFSQKSDLVKCQRTHTG.
(33) The sequence for the zinc finger consensus peptide that has two cysteines, one histidine, and then a third cysteine in the zinc-binding site (CP−CCHC) is: PYKCPECGKSFSQKSDLVKHQRTCTG.
(34) The sequence for the zinc-binding domain from the HIV-1 nucleocapsid protein (HIV−CCHC) is: VKCFNCGKEGHIARNCRA.
(35) Magyar, J. S.; Godwin, H. A. *Anal. Biochem.* **2003**, *320*, 39−54.
(36) Riddles, P. W.; Blakeley, R. L.; Zerner, B. *Methods Enzymol.* **1983**, *91*, 49−60.
(37) Clark-Baldwin, K.; Tierney, D. L.; Govindaswamy, N.; Gruff, E. S.; Kim, C.; Berg, J. M.; Koch, S. A.; Penner-Hahn, J. E. *J. Am. Chem. Soc.* **1998**, *120*, 8401−8409.
(38) Krizek, B. A.; Merkle, D. L.; Berg, J. M. *Inorg. Chem.* **1993**, *32*, 937−940.
(39) SPECFIT/32 is a product of Spectrum Software Associates and is owned solely by the authors Robert Binstead and Andreas Zuberbuhler.
(40) George, G. N.; Pickering, I. J. *EXAFSPAK: A Suite of Computer Programs for Analysis of X-ray Absorption Spectra*; SSRL: Stanford, CA, 1995.
(41) Zabinsky, S. I.; Rehr, J. J.; Ankudinov, A.; Albers, R. C.; Eller, M. J. *Phys. Rev. B* **1995**, *52*, 2995−3009.
(42) Ankudinov, A. L.; Ravel, B.; Rehr, J. J.; Conradson, S. D. *Phys. Rev. B* **1998**, *58*, 7565−7576.

Lundqvist potential and a self-consistent field calculation. Atomic absorption was calculated using the ground-state von Barth potential. A small core-hole broadening was used (0.5 eV) since larger values resulted in the disappearance of all edge features. For Pb−S_3 and Pb−S_2N clusters, a trigonal pyramidal geometry was assumed, with a distance of 0.5 Å from the metal to the basal plane of the ligands. Two structural models were considered for $Pb(aq)^{2+}$.[43−45] One structural model consisted of 12 waters (eight in square-prismatic coordination around Pb, plus a square-planar equatorial plane). In the other model, exclusion of the four planar oxygens gave a PbO_8 structure but gave a similar predicted XANES pattern for the same Pb−O distance.

Structure Determination of $[As(C_6H_5)_4]_4\{Pb[S_2C{=}C(CN)_2]_2\}_2$ (2). Single crystals of **2** were grown from ethanol/water by evaporation. A colorless needle crystal of $C_{112}As_4Pb_2N_8S_8H_{80}$ having approximate dimensions of 0.64 × 0.13 × 0.06 mm^3 was mounted on a glass fiber using oil (Infineum V8512). All measurements were made on a Bruker SMART-1000 CCD diffractometer with graphite monochromated Mo Kα radiation. Crystal data collection parameters are found in Table S1, Supporting Information. The data were collected at a temperature of 153 ± 1 K to a maximum 2θ value of 56.5°. Data were collected in 0.30° oscillations with 20.0 s exposures. The crystal-to-detector distance was 50.00 mm, and the detector swing angle was 28.00°. Of the 23 103 reflections which were collected, 11 622 were unique (R_{int} = 0.040); equivalent reflections were merged. Data were collected and processed using the SMART-NT and SAINT-NT programs (Bruker). A Gaussian face index absorption correction was applied (SHELXTL) with minimum and maximum transmission factors of 0.265 72 and 0.743 97, respectively. The data were also corrected for Lorentz and polarization effects.[46] The structure was solved by direct methods[47] and expanded using Fourier techniques.[48] The non-hydrogen atoms were refined anisotropically. Hydrogen atoms were included in idealized positions but not refined. The final cycle of full-matrix least-squares refinement on F^2 was based on 9228 observed reflections and 604 variable parameters and converged (largest parameter shift was 0.00 times its esd) with unweighted and weighted agreement factors of R = 0.028, R_w^2 = 0.054, respectively. The standard deviation of an observation of unit weight was 1.53. The maximum and minimum peaks on the final difference Fourier map corresponded to 1.29 and −1.26 e−/Å^3, respectively, and were located in the vicinity of the lead.

Neutral atom scattering factors were taken from Cromer and Waber.[46] Anomalous dispersion effects were included in F_{calc};[49] the values for $\Delta f'$ and $\Delta f''$ were those of Creagh and McAuley.[50] The values for the mass attenuation coefficients are those of Creagh and Hubbell.[51] All calculations were performed using the teXsan crystallographic software package of the Molecular Structure Corporation.[52]

Results

X-ray Absorption Spectroscopy of Pb−Peptides. To determine the coordination environment of lead bound to structural zinc-binding sites, X-ray absorption spectra of Pb(II) bound to each of four peptides that contained either three or four cysteine residues (CP−CCCC, CP−CCCH, CP−CCHC, and HIV−CCHC) were collected.[31−34] To determine the reproducibility of these measurements, X-ray absorption spectra were measured for each Pb−peptide species on at least three separate occasions, in each case using freshly prepared samples. Representative XANES spectra for each of the samples are shown in Figure 1. The XANES spectra are characterized by a broad, main transition at ca. 13 055 eV and are nearly identical for CP−CCCC and CP−CCCH, while the two CCHC peptides have a slightly different XANES spectrum. These spectra, particularly those for CCCC and CCCH, are typical of the XANES spectra seen for metal thiolates.[37] However, for each peptide, there was at least one spectrum with a significantly different structure, with the first peak being both lower in energy and more intense. The complete set of spectra is shown in Figure S1. The spectra in Figure 1 are all reproducible, with at least two identical spectra per sample. By contrast, the spectra with a low-energy first transition were more variable (see Figure S1), suggesting that, under some conditions, the Pb can adopt a different structure.

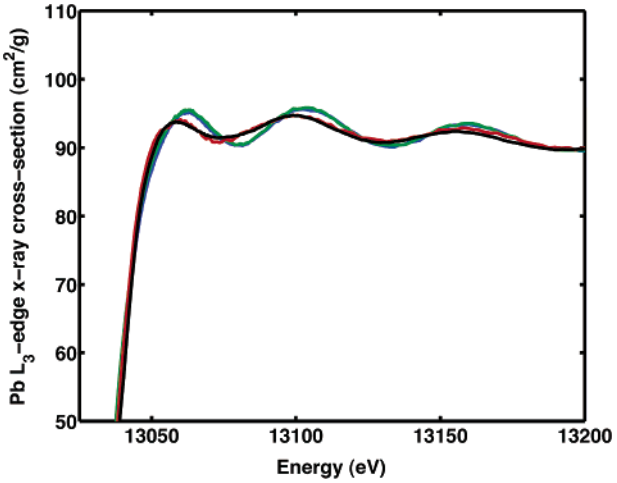

Figure 1. Normalized XANES spectra for the reproducible Pb−peptide complexes (see text; complete set of XANES spectra are included in Supporting Information). CP−CCCC (blue), CP−CCCH (green), CP−CCHC (red), HIV−CCHC (black).

The identity of these species is clarified by examination of the corresponding EXAFS spectra. The Fourier transforms of the reproducible subset of the EXAFS spectra for the Pb−peptide complexes are shown in Figure 2, with the EXAFS spectra themselves shown as an inset. In every case, these EXAFS spectra are dominated by a single frequency oscillation, indicating that the EXAFS is dominated by contributions from a single scatterer. All of these EXAFS spectra are well modeled by a single Pb−S shell with a Pb−S distance of 2.64 Å. The apparent Pb−S distance is identical for all of these samples to within the estimated precision of 0.003 Å.[53] By contrast, the EXAFS data for the nonreproducible spectra (see Supporting Information) are best modeled by a variable combination of Pb−S and Pb−(O/N) interactions. These "mixed" spectra could arise either from a combination of both Pb−S and Pb−(O/N) coordination around a single Pb (i.e., $Pb{-}S_x(O/N)_y$) or from a

(43) Rose, J.; Moulin, I.; Hazemann, J. L.; Masion, A.; Bertsch, P. M.; Bottero, J. Y.; Mosnier, F.; Haehnel, C. *Langmuir* **2000**, *16*, 9900−9906.
(44) Bargar, J. R.; Brown, G. E.; Parks, G. A. *Geochim. Cosmochim. Acta* **1997**, *61*, 2617−2637.
(45) Bargar, J. R.; Brown, G. E.; Parks, G. A. *Geochim. Cosmochim. Acta* **1997**, *61*, 2639−2652.
(46) Cromer, D. T.; Waber, J. T. *International Tables for X-ray Crystallography*; The Kynoch Press: Birmingham, England, 1974; Vol. IV, Table 2.2A.
(47) Sheldrick, G. M. *SHELX-97: Program for Crystal Structure Solution*; University of Göttingen: Göttingen, Germany, 1997.
(48) Beurskens, P. T.; Admiraal, G.; Beurskens, G.; Bosman, W. P.; de Gelder, R.; Israel, R.; Smits, J. M. M. *The DIRDIF-94 Program System*; Technical Report of the Crystallography Laboratory, University of Nijmegen: Nijmegen, The Netherlands, 1994.
(49) Ibers, J. A.; Hamilton, W. C. *Acta Crystallogr.* **1964**, *17*, 781.
(50) Creagh, D. C.; McAuley, W. J. *International Tables for Crystallography*; Kluwer Academic Publishers: Boston, 1992; Vol. C, pp 219−222, Table 4.2.6.8.
(51) Creagh, D. C.; Hubbell, J. H. *International Tables for Crystallography*; Kluwer Academic Publishers: Boston, 1992; Vol. C, pp 200−206, Table 4.2.4.3.
(52) *teXsan for Windows*, version 1.05; Molecular Structure Corporation: The Woodlands, TX, 1997−98.
(53) Riggs-Gelasco, P. J.; Mei, R.; Ghanotakis, D. F.; Yocum, C. F.; Penner-Hahn, J. E. *J. Am. Chem. Soc.* **1996**, *118*, 2400−2410.

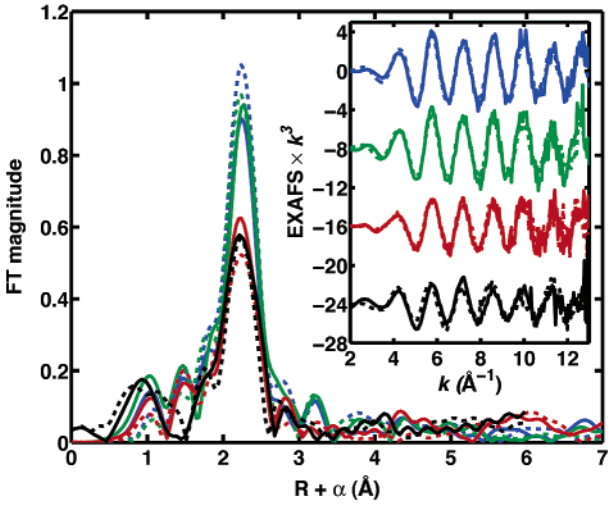

Figure 2. Fourier transforms (k^3-weighted) of EXAFS data (inset) for the "reproducible" Pb−peptide complexes. For each peptide, two independent samples (solid line and dashed line) are shown. CP−CCCC (blue), CP−CCCH (green), CP−CCHC (red), HIV−CCHC (black).

mixture of separate Pb−S_x and Pb−$(O/N)_y$ species. These two possibilities will be discussed further below. In either case, the erratic appearance of the "new" species appears to be a consequence of sample freezing, accounting for the nonreproducibility of these spectra.

Although the spectra in Figure 2 are all qualitatively similar, there is a nearly two-fold variation in the amplitude of the first FT peak. This variation indicates that there is some change in Pb environment between peptides. Even greater variation is seen if the Fourier transforms for the nonreproducible samples are included (see Figure S2), suggesting that there can also be significant variation in Pb environment between samples of a single peptide. The largest first FT peak amplitude is seen for FTs of the EXAFS data for Pb−CP−CCCC and Pb−CP−CCCH. These spectra are nearly identical and are well modeled using a single shell of three sulfurs with a relatively small Debye−Waller factor (see Table 1 for complete fitting results). There is no evidence for Pb coordination to nitrogen or oxygen ligands in either case, although it can be difficult to exclude definitively the presence of a small fraction of low-Z scatterers in the presence of sulfur scattering.[37] The observed Pb−S distance (2.64 Å) is slightly shorter than the 2.67 Å Pb−S distance found in the trigonal pyramidal model compound [(Tm^{Ph})Pb][ClO_4], **1**.[11] The short Pb−S distance and the fact that the data for CP−CCCC are identical to those for CP−CCCH, although the latter has only three sulfurs, strongly suggest that in both peptides the Pb is coordinated to only three cysteine sulfurs, even though four cysteine sulfurs are available for binding in CP−CCCC. The EXAFS spectrum for the other CP−CCCC sample (2001−5, see Figure S2) is well modeled as having only Pb−O ligation, with an apparent Pb−O coordination number of ca. 8 and a Pb−O distance of 2.61 Å. This result is consistent with the structure expected for a Pb-$(aq)^{2+}$ cation.

In the cases of Pb−CP−CCHC and Pb−HIV−CCHC, the spectra are somewhat less reproducible and in all cases have Fourier transforms that are less intense than those for CP−CCCC, indicating greater sample heterogeneity and likely Pb−peptide dissociation. The EXAFS data for CP−CCHC and HIV−CCHC can be modeled as a single shell of three sulfurs;

Table 1. Best Fits[a] to the EXAFS Data for CP and HIV Pb Samples

sample (year-month)	N_S[a]	R_S (Å)	$\sigma^2_S \times 10^3$ (Å²)	N_N	R_N (Å)	$\sigma^2_N \times 10^3$ (Å²)	F'[b]
CP−CCCC (2000-12)	3	2.638	2.9				0.31
CP−CCCC (2002-01)	3	2.640	3.4				0.37
CP−CCCH (2001-03)	3	2.644	2.8				0.75
CP−CCCH (2002-01)	3	2.644	3.4				0.87
CP−CCHC (2000-12)	3	2.640	4.7				0.42
	2	2.639	2.9	1	2.588	40	0.38
CP−CCHC (2001-03)	3	2.643	4.3				0.60
	2	2.641	4.3	1	2.486	16	0.59
HIV−CCHC (2000-12)	3	2.645	7.3				0.35
	2	2.646	4.5	1	2.570	4.1	0.36
HIV−CCHC (2002-04)	3	2.663	6.9				0.27
	2	2.646	4.9	1	2.575	2.1	0.26

[a] Coordination numbers were constrained to integer values. [b] F' is a reduced goodness-of-fit parameter.

however, a relatively large Debye−Waller factor is required to reproduce the data (Table 1). Alternatively, the data can be modeled as a mixture of Pb−S and Pb−(O/N) scatterers with nearly identical fit quality, but with a more reasonable Debye−Waller factor. These observations could result either from formation of a new bis-thiolato Pb complex in CP−CCHC and HIV−CCHC, or they could be the result of dissociation of a fraction of the Pb from the CP−CCHC and HIV−CCHC peptides to form $Pb(aq)^{2+}$. Either of these possibilities would give an average Pb environment of ca. Pb−$S_2(O/N)_1$, consistent with that seen in the EXAFS fits.

Low-temperature UV−visible absorption spectroscopy of the series of Pb−peptide complexes (discussed below) suggests that a $PbS_2(O/N)_1$ complex is not formed in CP−CCHC or HIV−CCHC. Further evidence against the formation of a bis-thiolato Pb−thiolate complex at low temperature comes from a more detailed examination of the XANES. The variability in the XANES spectra consistently involves a shift of the first XANES feature to lower energy and higher intensity (Figure 1). Simulations of the XANES spectra (Figure 3) using a Pb−S_3 model are able to reproduce the general shape of the XANES spectrum seen for CP−CCCC. If one of the thiolate ligands is exchanged for a nitrogen ligand, the simulated spectrum shows a shift to *higher* energy, in contrast with the observed shift to lower energy. However, simulations assuming an 8- or 12-coordinate Pb with oxygen ligation (intended to model Pb-$(aq)^{2+}$), show a shift to lower energy and higher amplitude, consistent with the spectra seen for the CCHC peptides. These results provide additional evidence that the variability in the XANES and EXAFS is best explained by formation of a small percentage of $Pb(aq)^{2+}$ when the samples are frozen.

Consistent with this explanation, we find that all of the X-ray absorption spectra can be described by a linear combination of the spectra for Pb−S_3 (e.g., the 2000−12 spectrum for CP−CCCC) and $Pb(aq)^{2+}$ (e.g., the 2001−5 spectrum for CP−CCCC); this is true both for the spectra from Table 1 and for the other, nonreproducible spectra. These fits, which are summarized in Table 2, suggest that the CP−CCHC and HIV−

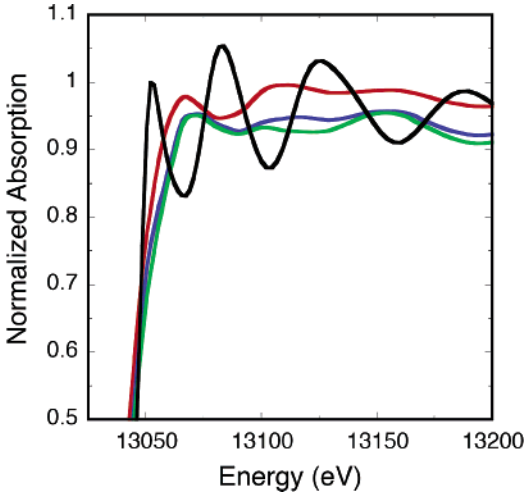

Figure 3. Simulated XANES spectra for Pb−S_3 (red, Pb−S = 2.64 Å); Pb−S_2N (green, Pb−S = 2.64 Å, Pb−N = 2.58 Å); Pb−S_2N + distant water (blue, Pb−S = 2.64 Å, Pb−N = 2.58 Å, Pb−O = 2.81 Å) and Pb−O_{12} (black, Pb−O = 2.75 Å). Pb−S and Pb−N distances taken from observed EXAFS (Table 1). The shift in XANES features to lower energy than is observed for the CCHC peptides (Figure 2) is not consistent with the conversion of Pb−S_3 into Pb−S_2N but is consistent with the presence of a small fraction of $Pb(aq)^{2+}$ cation.

Table 2. Apparent Percentage of Pb−S_3 in CCHC Peptides[a]

	sample date (year-month)				
peptide	2000-12	2001-03	2001-05	2002-01	2002-04
CP−CCHC EXAFS	80.8	75.6	49.9	26.5	2.1
CP−CCHC XANES	90.6	82.7	54.5	28.5	0.0
HIV−CCHC EXAFS	70.0	45.5	44.1	NA[b]	66.3
HIV−CCHC XANES	79.2	66.7	62.0	NA[b]	79.9

[a] The percentage of Pb−S_3 (CP−CCCC-2000−12) giving the best fit when unknown spectra were fit as linear combinations of Pb−S_3 and $Pb(aq)^{2+}$ (CP−CCCC-2001-5) spectra. [b] Not available.

CCHC samples contain between 30% and 90% Pb−S_3, with the spectra from Table 1 representing the high end of this range. Nearly identical results are obtained using the XANES region or the k^3-weighted EXAFS region. Taken together, these results suggest that for all four peptides, the peptide-coordinated Pb(II) is three-coordinate, bound to three (and only three) cysteines and that some of the peptides, particularly those with the CCHC metal binding sequence, are prone to dissociation of a fraction of the Pb.

Loss of lead from the peptide may represent intrinsic instability. However, no such instability is observed in room-temperature UV−visible spectra or spectrometric titrations, suggesting that instead this dissociation may be a consequence of sample freezing.

Low-Temperature UV−visible Absorption Spectroscopy of Pb−Peptides. To evaluate whether the electronic spectral features observed at room temperature persist upon sample freezing, UV−visible absorption spectra were collected at low temperature (~4 K) for apo- and Pb-bound HIV−CCHC, CP−CCHC, CP−CCCH, and CP−CCCC. For the apo-peptides (Figure S4), the primary features in the electronic spectra of the three consensus peptides (CP−CCCC, CP−CCCH, CP−CCHC) are bands at 276 and 282 nm, attributed to absorption by the aromatic residues, i.e., tyrosine and phenylalanine.[31−33] The absorbance in this region of the apo-HIV−CCHC spectrum is diminished and featureless as the peptide contains no tyrosine and only a single phenylalanine residue.[34] In general, the electronic features of the apo-peptides appear as shoulders in the uncorrected spectra of the Pb-bound peptides (Figure 4).

In the room-temperature electronic absorption spectra of all four Pb−peptide complexes there are two bands: an intense absorption at ca. 255 nm ($\epsilon \approx 16\,000$ M^{-1} cm^{-1}) and a less intense feature at ca. 330 nm ($\epsilon \approx 4000$ M^{-1} cm^{-1}) (Figure 4).[13] These transitions contain both ligand-to-metal charge-transfer (S 3p → Pb 6p) and intraatomic (Pb $6s^2$ → Pb 6sp) character (for Pb in O_h: $a_{1g}^{*\,2} \rightarrow a_{1g}^{*\,1}\, t_{1u}^{*\,1}$).[54−58] The electronic features persist in spectra obtained at 4 K (Figure 4); all four species exhibit transitions at ~320−325 nm (A-Band) and ~255−260 nm (B-Band). The absorption maximum of the low-energy feature in each spectrum is blue-shifted by ~5−10 nm relative to the corresponding spectrum at room temperature, with a slightly greater blue shift for Pb−CP−CCHC and Pb−HIV−CCHC, but the general absorption profiles for all of the Pb−peptides are essentially the same. The relatively small blue shift in the 325 nm transition (~750 cm^{-1}) can be readily explained by the transition from solution to frozen glass (i.e., the inability of solvent dipoles to stabilize the excited state as effectively),[59] suggesting that Pb−S_3 coordination remains intact and partial Pb−peptide ligand dissociation (Pb−S_3 → Pb−S_2) is not occurring. It is true, however, that thiolate ligand dissociation would generate a blue shift in the charge-transfer transitions: for $[PbBr_4]^{2-} \rightarrow [PbBr_3]^{-} + Br^{-}$ the A-band blue shifts ca. 3500 cm^{-1} and the extinction increases by a factor of ca. 3.5.[58] The energy shift suggests differential stabilization of the t_{1u}^* and a_{1g}^* model orbitals (a_{1g}^* having greater σ-character) upon ligand loss. This scenario is in contrast to the more common case where loss of a ligand leads to a decrease in energy of the LMCT band (by ca. 3000−4000 cm^{-1}) attributable to the ligand-donor-bonding → metal-*d*-antibonding nature of the transition.[60−62] Thus the small blue shifts observed for the Pb−peptides are not consistent with loss of a thiolate ligand. Moreover, changes in the extinction coefficient of the charge-transfer transition should be observed if ligand dissociation occurs. For Pb−CP−CCCH and Pb−CP−CCCC we have estimated the extinction coefficients for the A-band to be ca. 3700−4300 M^{-1} cm^{-1} at 4 K, similar to the value at ambient temperature.[13] For Pb−HIV−CCHC and Pb−CP−CCHC, the extinction is somewhat reduced (ca. 1800−2200 M^{-1} cm^{-1}), despite the similarity to the other Pb−peptides in the energy of the transition.

The electronic absorption spectra suggest that the Pb−peptide species observed at room temperature generally persist at the low temperatures used for XAS and support the interpretation of the EXAFS and XANES data in which all of the peptides exhibit Pb−S_3 coordination. The decrease in amplitude without

(54) Claudio, E. S.; Godwin, H. A.; Magyar, J. S. *Prog. Inorg. Chem.* **2003**, *51*, 1−144.
(55) Couch, D. A.; Wilkins, C. J.; Rossman, G. R.; Gray, H. B. *J. Am. Chem. Soc.* **1970**, *92*, 307−310.
(56) Vogler, A.; Nikol, H. *Pure Appl. Chem.* **1992**, *64*, 1311−1317.
(57) Bramanti, D.; Mancini, M.; Ranfagni, A. *Phys. Rev. B* **1971**, *3*, 3670−3676.
(58) Oldenburg, K.; Vogler, A. *Z. Naturforsch.* **1993**, *48b*, 1519−1523.
(59) Ghoneim, N.; Rohner, Y.; Suppan, P. *Faraday Discuss. Chem. Soc.* **1988**, *86*, 295−308.
(60) Basumallick, L.; George, S. D.; Randall, D. W.; Hedman, B.; Hodgson, K. O.; Fujisawa, K.; Solomon, E. I. *Inorg. Chim. Acta* **2002**, *337*, 357−365.
(61) Gamelin, D. R.; Randall, D. W.; Hay, M. T.; Houser, R. P.; Mulder, T. C.; Canters, G. W.; de Vries, S.; Tolman, W. B.; Lu, Y.; Solomon, E. I. *J. Am. Chem. Soc.* **1998**, *120*, 5246−5263.
(62) Lever, A. B. P. *J. Chem. Educ.* **1974**, *51*, 612−616.

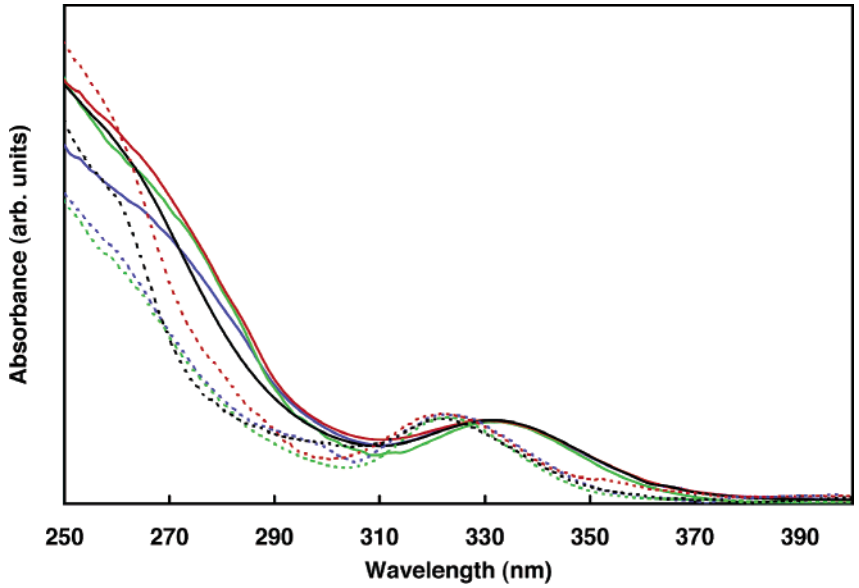

Figure 4. UV−visible absorption spectra of Pb−peptides at room temperature (~298 K, solid lines) and low temperature (~4 K, dashed lines). Pb−CP−CCCC (blue), Pb−CP−CCCH (green), Pb−CP−CCHC (red), Pb−HIV−CCHC (black). The spectrum of the apopeptide (Supporting Information, Figure S4) has not been subtracted.

Table 3. Absolute and Relative Binding Affinities for Pb(II) and Zn(II) to Thiol-Rich Sites

peptide	log K_b^{Co}	log K_b^{Zn}	log K_b^{Pb}	log [K_b^{Pb}/K_b^{Zn}]	reference
HIV−CCHC	7.0	10.2	9.5	−0.6	13, 38
CP−CCHC	7.2	11.5	10.1	−1.4	13, 38
CP−CCCH	7.2	10.5	10.9	0.4	this work
CP−CCCC	6.5	12.0	13.4	1.5	13, 38
Tm^{Ph}	nd[a]	nd	nd	2.7	11

[a] nd = not determined.

shift in energy of the S^{2-}-to-Pb^{2+} charge-transfer transitions in the spectra of Pb−HIV−CCHC and Pb−CP−CCHC also suggests some degree of complete Pb(II) dissociation (and formation of $Pb(aq)^{2+}$) upon freezing; the presence of $Pb(aq)^{2+}$ would not lead to a new charge-transfer transition or a shift in the existing A-band energy. The formation of some $Pb(aq)^{2+}$ is also consistent with EXAFS and XANES structural analyses.

Metal-Binding Titrations of CP−CCCH. Although the metal-binding thermodynamics of the CP−CCHC and CP−CCCC consensus peptides have been examined previously,[13,38] no information was available for the CP−CCCH peptide. Therefore, we conducted a series of titrations to determine the metal−CP−CCCH binding constants for Co(II), Zn(II), and Pb-(II) (Table 3). These results reveal some intriguing differences among the peptides, particularly in relative metal-binding affinities. Although the Co(II)-affinity of CP−CCCH is identical to that of CP−CCHC (and quite close to that of CP−CCCC), the affinity of CP−CCCH for Zn(II) is an order of magnitude less than that of CP−CCHC. By contrast, CP−CCCH binds Pb(II) almost an order of magnitude *more* tightly than CP−CCHC, although still much less tightly than CP−CCCC does.

By contrast K_b^{Co} is identical for CP−CCHC and CP−CCCH; this is not surprising because a major contribution to the stability (or instability) of these complexes comes from the decreased ligand field stabilization energy (LFSE) on changing from octahedral hexaaqua Co(II) to tetrahedral Co(II) in the peptide; the LFSE contribution is equivalent for CP−CCHC and CP−CCCH.[38,63] The role of LFSE also accounts for the dramatically higher affinity of these peptides for Zn(II) (which is d^{10} and therefore has no LFSE) over Co(II) (d^7).[38,63]

LFSE effects, however, can account neither for the relative destabilization of Zn(II) in CP−CCCH vs CP−CCHC nor for the relative affinities of Zn(II) (d^{10}) and Pb(II) ($d^{10}s^2$). In these cases, the ligand type and position in the peptide must have the dominant effect.

The key differences in the metal affinities of CP−CCHC, CP−CCCH, and CP−CCCC are highlighted in Table 3. Strikingly, CP−CCCH, like CP−CCCC and unlike CP−CCHC and HIV−CCHC, has a greater affinity for Pb(II) than for Zn-(II). The absolute affinity of CP−CCCH for Pb(II) is also greater than that of CP−CCHC or HIV−CCHC. These results are consistent with the greater apparent stability of the Pb−CP−CCCH XAS samples; significant Pb(II) dissociation was observed upon freezing CP−CCHC and HIV−CCHC but not CP−CCCH or CP−CCCC.

The differences in metal ion affinity for the three consensus peptides imply that the positions of the metal-binding amino acids in the peptide, and not simply the number of ligands, affect the strength of metal coordination. Since the XAS of Pb−CP−CCCC and Pb−CP−CCCH reveal identical $Pb-S_3$ coordination but nevertheless the two peptides have quite different Pb binding constants, it seems likely that the first three cysteines in the peptide sequence are not in the most favorable positions for Pb binding, i.e., that these are not the three cysteines that are coordinated to the Pb in Pb−CP−CCCC. The affinity of CP−CCHC for Pb is even worse. An examination of the peptide sequence reveals that there are only two residues (one of which is a proline) between the first two cysteines.[31−33] We suggest that these two cysteines are too close together for ideal trigonal pyramidal symmetry around the Pb(II), thus destabilizing the complex. The effective ionic radius of Pb^{2+} (0.98 Å) is significantly larger than that of Zn^{2+} (0.60 Å).[64] In the case of CP−CCHC, perhaps the complex is even further destabilized

(63) Berg, J. M.; Merkle, D. L. *J. Am. Chem. Soc.* **1989**, *111*, 3759−3761.
(64) Shannon, R. D. *Acta Crystallogr.* **1976**, *A32*, 751−767.

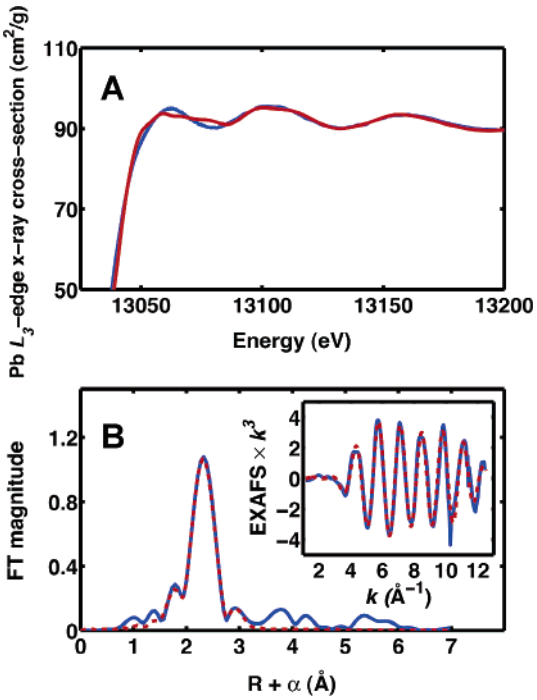

Figure 5. X-ray absorption data for [(Tm^{Ph})Pb][ClO_4]. (A) XANES spectra showing minor differences between the XANES for [(Tm^{Ph})Pb][ClO_4] (red) and that for Pb−CP−CCCC (blue). (B) Fourier transform of the EXAFS data for [(Tm^{Ph})Pb][ClO_4]. The filtered first shell data (blue solid line) can be well described using only a Pb−S shell (red dashed line).

by the particularly long loop (16 amino acids) between the last two cysteines. Without tetrahedral metal coordination to guide it, this loop is unstructured. The longest unstructured loop is only 12 amino acids in the CP−CCCH case.

We would predict from these results, then, that a peptide with the consensus peptide (CP) sequence but with a XCCC metal-binding site[65] will have a greater Pb-affinity than either CP−CCCH or CP−CCHC and will likely have an affinity near that of CP−CCCC. In the case of CP−CCCC, it is not the presence of a fourth cysteine ligand that leads to tight binding; rather, it is the presence of three cysteine ligands in positions favorable for the formation of a trigonal pyramidal complex.

Lead Model Compounds. To calibrate our EXAFS fits, and as references for interpretation of our XANES, we measured X-ray absorption spectra of two Pb(II) model compounds. The tris(2-mercapto-1-phenylimidazolyl)hydroborato lead complex, [(Tm^{Ph})Pb][ClO_4] **1**, was originally prepared as a Pb−S_3 model for Pb(II) bound to 5-aminolevulinate dehydratase (ALAD), an enzyme on the heme biosynthesis pathway that is known to be inhibited by lead.[8,9,11] In **1**, as in Pb-ALAD, the lead is coordinated to three sulfurs with trigonal pyramidal geometry. There is no fourth ligand to the Pb in **1**, although an oxygen from the perchlorate counterion is relatively close to the Pb(II) (Pb−O = 2.94 Å).[11] The XANES of **1** is very similar to that for Pb−CP−CCCC (Figure 5A) although there are small differences in the lowest energy portion of the spectrum. As with the peptide EXAFS data, the EXAFS of **1** (Figure 5B) can be fit with a shell of three sulfurs, with a Pb−S bond length (2.671 Å) that compares favorably to that determined by X-ray diffraction (2.693 Å). However, in contrast to the peptide data, it was not possible to obtain a good fit using only the Pb−S shell; we

(65) For example, PYKHPECGKSFSQKSDLVKCQRTCTG

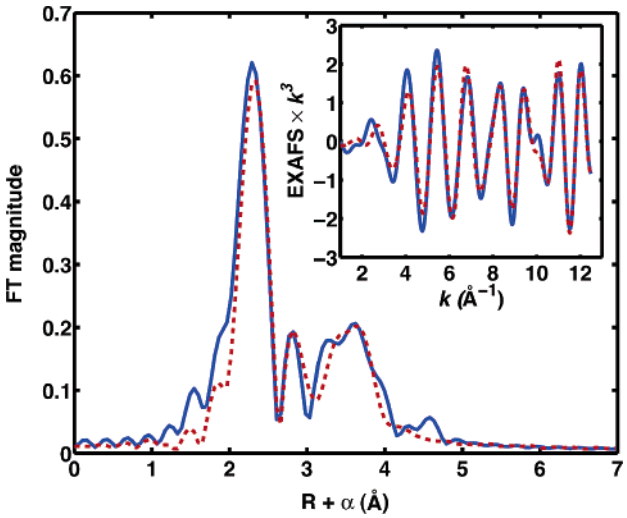

Figure 6. EXAFS data and k^3-weighted Fourier transforms for [Pb(i-mnt)$_2$]$_2^{4-}$. A single-shell model was used to give the best fit (red dashed line) to the raw data (blue solid line).

attribute this difference to weak contributions from the perchlorate oxygen.

As a model for a possible Pb−S_4 site, we synthesized a standard "Pb(II)-S_4" complex from the literature: tetraphenylarsonium lead(II) *iso*-maleonitriledithiolate, **2**.[29] This compound was not only described as a Pb−S_4 complex, **2b** (with a distorted square-pyramidal geometry),[29] but was also cited in a recent review as an example of a typical hemidirected tetrahedral geometry, produced by a stereochemically active lone pair at the top of the square pyramid.[66] However, a new high-resolution crystal structure of the complex along with data from X-ray absorption spectroscopy have led us to a new interpretation of this structure (**2a**).[29]

The X-ray absorption spectrum of **2** (Figure 6) showed the expected first-shell peak attributable to Pb−S scattering. This peak was well fit using a shell of Pb−S at 2.744 Å. However, the best fit was obtained using three sulfur scatterers, rather than the expected four sulfur scatterers. More disconcertingly, the EXAFS data showed clear evidence for at least two shells of strong outer shell scattering. A peak at ca. 2.7 Å can be modeled as Pb−C scattering from the *iso*-maleonitriledithiolate (*i*-mnt) ligand or as a long Pb−S interaction, either at ∼3 Å from the Pb. However, the peak at higher (R + α) could only be modeled by including a Pb−Pb interaction at 3.70 Å. As these outer shell interactions were not described in the original crystallographic report, we considered the possibility that we had obtained a new structure of the [Pb(*i*-mnt)$_2$]$^{2-}$ anion, and thus we determined the structure of a single crystal that was grown from the same powder that had been used for the XAS measurements. The resulting crystal structure turned out to be a redetermination of the reported structure of **2**; however, the structure was much better determined (R = 0.028) than previously (R = 0.0652). Careful examination of the crystal packing for this structure shows that, in fact, the complex is a dimer with bridging sulfur atoms (Figure 7), not a monomer as originally described.[29] The interatomic distances calculated from the EXAFS are in reasonable agreement with the average distances in the crystal structure (Table S2).

(66) Shimoni-Livny, L.; Glusker, J. P.; Bock, C. W. *Inorg. Chem.* **1998**, *37*, 1853−1867.

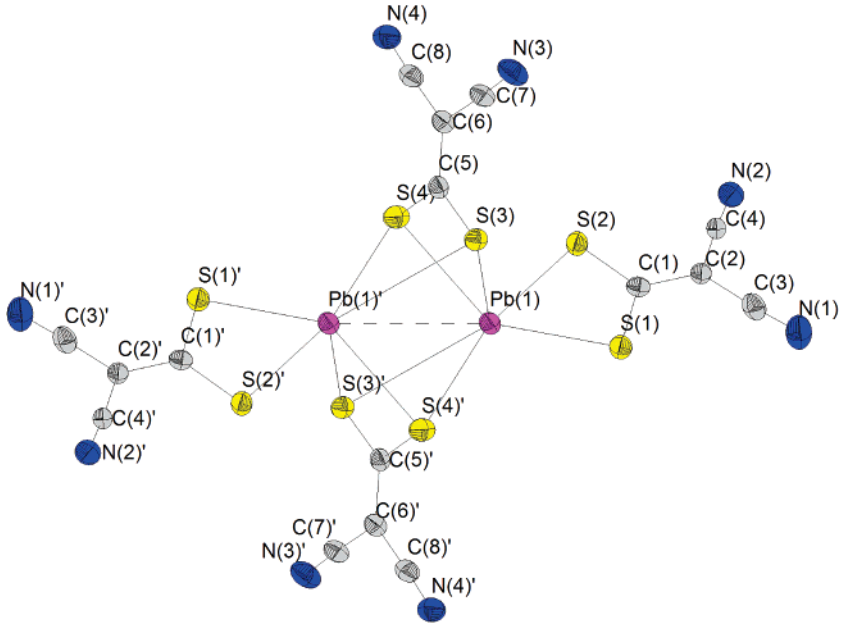

Figure 7. X-ray crystal structure of $[AsPh_4]_4[Pb(i\text{-mnt})_2]_2$. Thermal ellipsoids are set at 50% probability; for clarity, the $AsPh_4$ cations are not shown.

Each Pb(II) atom in the dimer is six-coordinate, with three short Pb−S distances (2.704, 2.764, 2.857 Å) and three longer Pb−S distances (3.003, 3.268, 3.597 Å). All of these distances are within the sum of the Pb and S van der Waals radii (3.8 Å).[67] The Pb $6s^2$ lone pair likely contributes significantly to the distortion from regular octahedral geometry, but each lead is not four-coordinate as originally reported; rather, it is *six*-coordinate. The $[Pb(i\text{-mnt})_2]_2^{4-}$ dimer resides on a crystallographic inversion center, with the asymmetric unit composed of a mononuclear hemidirected $[Pb(i\text{-mnt})_2]^{2-}$ fragment (Figure 7), which is presumably the reason that the dimeric nature of the complex was overlooked in the original report. The dinuclear nature of **2** is discussed by Caruso et al., but they exclude the longest Pb−S interaction and report an overall five-coordinate Pb.[68] In the original report, the longest Pb−S distance is 3.70 Å;[29] the distance is slightly shorter in our redetermined structure (3.597 Å) and should be included in the coordination sphere.[69]

Previously, Caruso et al. had concluded that there is no bond between the two Pb atoms in **2**; they argued that the difference in bond lengths between "primary" and "secondary" Pb−S bonds excludes complete donation of the Pb(II) lone pair to the neighboring metal.[68] Nevertheless, the Pb−Pb distance (3.697 Å) in $[Pb(i\text{-mnt})_2]_2^{4-}$ is only somewhat longer than a typical Pb−Pb bond (the Pb−Pb distance in metallic lead is 3.50 Å; the Pb−Pb distances in $Pb_6O(OH)_6^{4+}$ range from 3.44 to 4.09 Å)[70] and is within the sum of the van der Waals radii (4.04 Å).[67] In a related system, Trinquier and Hoffmann concluded that the chains and layers in both α- and β-PbO are held together by real, although weak, Pb−Pb bonds, not just van der Waals interactions; the Pb−Pb distances in PbO are 3.47 to 3.97 Å.[71] Even if a *bona fide* Pb−Pb bond does not exist, a weak interaction between the lead centers is not precluded. In the case of $[Pb(i\text{-mnt})_2]_2$,$^{4-}$ we observe that the Pb−Pb interaction is readily detectable in the low-temperature EXAFS data, which provides clear evidence that there is a strong correlation in atomic motion between the two lead atoms. Although we are not aware of any examples to date of biologically relevant lead dimers, these data demonstrate that should a thiolate-bridged Pb dimer exist in a protein, the Pb−Pb interaction should be readily detectable. We do not observe this interaction in our Pb−peptide species, consistent with a model in which lead forms a 1:1 monomeric complex with each of these peptides.

Discussion

The studies reported here were initiated to elucidate why lead does not promote proper folding of structural zinc-binding domains. We determined the coordination mode of lead when it is bound to peptides containing $Cys_2HisCys$, Cys_3His, or Cys_4 structural-zinc binding sites, investigating these sites in the context of two different protein frameworks: a consensus zinc-finger peptide (CP) and a single domain from HIV nucleocapsid protein (HIV).[38,72] Previous studies had revealed that Pb(II) binds tightly to the $Cys_2HisCys$ and Cys_4 sites but binds more tightly to the Cys_4 site in CP−CCCC (log $K_b^{Pb} = 13.6$) than to the $Cys_2HisCys$ sites in either CP−CCHC (log $K_b^{Pb} = 10.1$) or HIV−CCHC (log $K_b^{Pb} = 9.5$) (Table 3). The simplest interpretation of these results was that lead assumes different coordination modes in these two sites (e.g., S_4 vs S_3O/N) and that the presence of the fourth cysteine in the CP−CCCC peptide confers tighter lead binding. However, the room-temperature UV−vis spectra of all three of the lead−peptide complexes are identical (Figure 4).[13] Because these absorption bands result in part from S 3p → Pb 6p LMCT,[54] we would expect the energy of the bands to red-shift for lead bound to sites with fewer lead−thiolate bonds. In fact, no variation between sites is observed at room temperature, and a very small *blue* shift is observed at low temperature.[73]

(67) Bondi, A. *J. Phys. Chem.* **1964**, *68*, 441−451.
(68) Caruso, F.; Chan, M.-L.; Rossi, M. *Inorg. Chem.* **1997**, *36*, 3609−3615.
(69) It should be noted that Caruso et al. 1997 also discuss the importance of long-range Pb−S interactions in several other related structures.
(70) Spiro, T. G.; Templeton, D. H.; Zalkin, A. *Inorg. Chem.* **1969**, *8*, 856−861.
(71) Trinquier, G.; Hoffmann, R. *J. Phys. Chem.* **1984**, *88*, 6696−6711.
(72) South, T. L.; Summers, M. F. *Protein Sci.* **1993**, *2*, 3−19.
(73) Wrighton, M.; Morse, D. L. *J. Am. Chem. Soc.* **1974**, *96*, 998−1003.

To determine whether the lead−thiolate coordination number varied between the Cys_4 and $Cys_2HisCys$ peptides, we investigated the lead−peptide complexes using XAS. Surprisingly, the XAS data obtained for Pb−CP−CCCC are best fit with a model in which the central Pb(II) is bound by three S atoms at 3.638 Å (Figures 1, 2). Furthermore, the X-ray absorption spectrum of Pb−CP−CCCC is nearly identical to that obtained for the model compound **1** (Figure 5), which contains Pb bound to three sulfur atoms in a trigonal pyramidal mode (Pb−S distance = 2.693(2) Å).[11] These data suggest that in CP−CCCC, Pb(II) only binds to three of the four available cysteines. Pb−CP−CCHC and Pb−HIV−CCHC exhibit FTs of the EXAFS scattering peaks at the same distance as Pb−CP−CCCC, but with lower, and less reproducible, intensity. These data can be fit using two different models: one in which there is a mixture of $Pb-S_3$ and $Pb-(OH_2)_x$ present in solution and one in which there is a homogeneous solution of a $Pb-S_2(O/N)$ compound in solution. Results from low-temperature absorption spectroscopy and XANES simulations are most consistent with the model in which lead assumes a $Pb-S_3$ coordination mode in all four peptides examined, but the Pb−CP−CCHC and Pb−HIV−CCHC complexes are less stable than Pb−CP−CCCC, particularly at low temperature.

The results suggest that the relative *positions* of the three cysteine residues in the peptides are critical to the stability of the $Pb-S_3$ complex. To test this hypothesis, we prepared a different permutation of the CP−CCHC peptide: CP−CCCH. Quantitative Pb-binding titrations revealed that this variant does indeed bind lead more tightly ($\log K_b^{Pb} = 10.9$) than CP−CCHC ($\log K_b^{Pb} = 10.1$). Furthermore, the X-ray absorption and low-temperature UV−vis spectra of Pb−CP−CCCH are virtually superimposable with those of Pb−CP−CCCC.

The observation that Pb assumes a preferred coordination mode of $Pb-S_3$ *even when an additional thiolate is available for binding* appeared to contradict several reports in the literature stating that Pb(II) assumes a tetrahedral $Pb-S_4$ coordination mode in thiol-rich small molecules.[29,30,74,75] Experimental reexamination of one of the classic "$Pb-S_4$" compounds, **2**, using X-ray absorption spectroscopy and X-ray crystallography revealed that the original structure had been misinterpreted: the compound actually exists as a $[Pb(i\text{-}mnt)_2]_2^{4-}$ dimer in the solid state, with each Pb(II) assuming a distorted six-coordinate geometry.

Upon discovering this misinterpretation, we conducted a comprehensive survey of the existing crystallographic literature on small molecules containing multiple Pb−S bonds. Even though Pb(II) is generally considered to be thiophilic, only 35 of the 1026 total Pb structures recorded in the Cambridge Structural Database[76] have an inner coordination sphere composed entirely of sulfur atoms.[77] The dearth of well-characterized Pb−S compounds makes generalizations about lead's preferred ligand geometry and coordination difficult at best. Of those 35 compounds, however, only one has true $Pb-S_4$ coordination.[78] Although some of the remaining structures were reported to be four-coordinate, all actually have Pb coordination numbers either ≤ 3 or ≥ 5.[11,29,68,75,79−105] In all the cases (but one) where Pb would be expected to be four-coordinate, the metal ion actually interacts with the ligands of the neighboring molecule(s) in the crystal, forming an extended structure or coordination polymer.[106] These supramolecular interactions result in increased coordination numbers for lead, generally 5, 6, or 8. A number of researchers have recognized the existence of these secondary Pb−S interactions;[68,79−91] such interactions also appear in several other crystallographically characterized compounds but were not noted.[29,30,75,101] The one truly four-coordinate compound in the database is lead(II) bis{2,6-bis[bis(trimethylsilyl)methyl]-4-[tris(trimethylsilyl)methyl]phenyl trithiocarbonate}.[78] The Pb(II) in this complex is forced into four-coordination by the extreme bulk of the ligands; the lead is so buried within the ligands that it cannot form an extended structure. By contrast, several $Pb-S_3$ complexes without these intermolecular Pb−S interactions are known.[11,92,94]

It has been asserted in the literature that the most common coordination numbers for Pb(II) are 4 and 6.[66] For Pb(II) in all-sulfur coordination, however, this is not the case. Our results, in fact, show a clear preference for Pb(II) to *avoid* four-coordination, adopting three-coordination in solution or higher coordination numbers in the solid state, where possible. Lead

(74) Carrell, H. L.; Glusker, J. P.; Shimoni, L.; Keefe, L. J.; Afshar, C.; Volin, M.; Jaffe, E. K. *Acta Crystallogr.* **1996**, *D52*, 419−421.
(75) Hummel, H.-U.; Meske, H. *Z. Naturforsch.* **1989**, *44b*, 1531−1537.
(76) Allen, F. H.; Bellard, S.; Brice, M. D.; Cartwright, B. A.; Doubleday: A.; Higgs, H.; Hummelink, T.; Hummelink-Peters, B. G.; Kennard, O.; Motherwell, W. D. S.; Rodgers, J. R.; Watson, D. G. *Acta Crystallogr.* **1979**, *B35*, 2331−2339.
(77) The January 2004 version of the CCDC database (version 5.25 with one update) was searched using Conquest 1.6. The database was searched for compounds containing Pb with an *R*-factor ≤ 0.075; a total of 1026 compounds was found.
(78) Kano, N.; Tokitoh, N.; Okazaki, R. *Organometallics* **1998**, *17*, 1241−1244.
(79) Harrison, P. G.; Steel, A.; Pelizzi, G.; Pelizzi, C. *Main Group Met. Chem.* **1988**, *11*, 181−204.
(80) Silvestru, C.; Haiduc, I.; Cea-Olivares, R.; Hernández-Ortega, S. *Inorg. Chim. Acta* **1995**, *233*, 151−154.
(81) Casas, J. S.; Castiñeiras, A.; Haiduc, I.; Sànchez, A.; Sordo, J.; Vàzquez-Lòpez, E. M. *Polyhedron* **1994**, *13*, 2873−2879.
(82) Baba, I.; Farina, Y.; Othman, A. H.; Razak, I. A.; Fun, H.-K.; Ng, S. W. *Acta Crystallogr.* **2001**, *E57*, m35−m36.
(83) Rae, A. D.; Craig, D. C.; Dance, I. G.; Scudder, M. L.; Dean, P. A. W.; Kmetic, M. A.; Payne, N. C.; Vittal, J. J. *Acta Crystallogr.* **1997**, *B53*, 457−465.
(84) Lawton, S. L.; Kokotailo, G. T. *Inorg. Chem.* **1972**, *11*, 363−368.
(85) Trindade, T.; O'Brien, P.; Zhang, X.-m.; Motevalli, M. *J. Mater. Chem.* **1997**, *7*, 1011−1016.
(86) Iwasaki, H. *Acta Crystallogr.* **1980**, *B36*, 2138−2139.
(87) Ito, M.; Iwasaki, H. *Acta Crystallogr.* **1980**, *B26*, 443−444.
(88) Ebert, K. H.; Breunig, H. J.; Silvestru, C.; Stefan, I.; Haiduc, I. *Inorg. Chem.* **1994**, *33*, 1695−1699.
(89) Tiekink, E. R. T. *Acta Crystallogr.* **1988**, *C44*, 250−253.
(90) Dance, I. G.; Guerney, P. J.; Rae, A. D.; Scudder, M. L.; Baker, A. T. *Aust. J. Chem.* **1986**, *39*, 383−398.
(91) Dean, P. A. W.; Vittal, J. J.; Payne, N. C. *Inorg. Chem.* **1985**, *24*, 3594−3597.
(92) Dean, P. A. W.; Vittal, J. J.; Payne, N. C. *Inorg. Chem.* **1984**, *23*, 3.
(93) Hitchcock, P. B.; Lappert, M. F.; Samways, B. J.; Weinberg, E. L. *Chem. Commun.* **1983**, 1492−1494.
(94) Christou, G.; Folting, K.; C., H. J. *Polyhedron* **1984**, *3*, 1247−1253.
(95) Hardin, S. G.; Healy, P. C.; Mumme, W. G.; White, A. H.; Winter, G. *Aust. J. Chem.* **1982**, *35*, 2423−2433.
(96) Borrmann, H.; Campbell, J.; Dixon, D. A.; Mercier, H. P. A.; Pirani, A. M.; Schrobilgen, G. J. *Inorg. Chem.* **1998**, *37*, 6656−6674.
(97) Bharadwaj, P. K.; Arbuckle, B. W.; Musker, W. K. *Inorg. Chim. Acta* **1988**, *142*, 243−246.
(98) Perez-Lourido, P.; Romero, J.; Garcia-Vazquez, J. A.; Sousa, A.; Zheng, Y.; Dilworth, J. R.; Zubieta, J. *J. Chem. Soc., Dalton Trans.* **2000**, 769−774.
(99) Ng, S. W. *Acta Crystallogr.* **1999**, *C55*, 9900091.
(100) Hummel, H.-U.; Meske, H. *Z. Naturforsch.* **1988**, *43b*, 389−398.
(101) Chekhlov, A. N. *Russ. J. Coord. Chem.* **2000**, *26*, 239−243.
(102) Muller, A.; Bogge, H.; Schimanski, U.; Penk, M.; Nieradzik, K.; Dartmann, M.; Krickemeyer, E.; Schimanski, J.; Romer, C.; Romer, M.; Dornfield, H.; Wienboker, U.; Hellmann, W.; Zimmermann, M. *Monatsh. Chem.* **1989**, *120*, 367−391.
(103) Svensson, G.; Albertsson, J. *Acta Chem. Scand.* **1991**, *45*, 820−827.
(104) Bridgewater, B. M.; Parkin, G. *Inorg. Chem. Commun.* **2000**, *3*, 534−536.
(105) Heinl, U.; Hinse, P.; Frohlich, R.; Mattes, R. *Z. Anorg. Allg. Chem.* **2002**, *628*, 770−778.
(106) Harrowfield, J. M.; Shahverdizadeh, G. H.; Soudi, A. A. *Supramol. Chem.* **2003**, *15*, 367−373.

complexes with stereochemically active lone pairs are often simply described as "distorted" in structure; this is likely a superficial description. The results of the studies described here indicate that Pb(II) prefers to *avoid* $Pb-S_4$ coordination whenever possible by binding with either a trigonal pyramidal (three-coordinate) or higher-coordinate (≥ 5) geometry. In solution, Pb(II) appears to opt for lower coordination and trigonal pyramidal geometry; in the solid state, crystal packing forces likely contribute dramatically to the preference for higher coordination.

A similar preference of Pb(II) for Pb(II)-S_3 coordination has been reported by Giedroc and co-workers for the metalloregulatory protein CadC based on studies by optical and X-ray absorption spectroscopies.[107,108] The thiolate-rich primary metal-binding site of apo-CadC binds Cd(II) and Bi(III), and possibly Zn(II) and Co(II), with a distorted tetrahedral geometry (e.g., Cd(II)-S_4). By contrast, Pb(II) is trigonal (i.e., Pb(II)-S_3) in the same site.[108,109] Once again, the mere presence of additional thiolate ligands does not lead to increased Pb(II) coordination.

Our work with the series of zinc finger consensus peptides demonstrates that Pb(II) binds with different coordination than Zn(II), which can have a dramatic effect on protein folding and ability to function. Pb(II), owing to its natural thiophilicity, binds tightly to a variety of sulfur-rich protein sites, including GATA proteins and steroid receptor DNA-binding domains.[14,110,111] Furthermore, Pb(II) replaces Zn(II) in these proteins under physiologically relevant conditions, and Pb(II) binding diminishes protein function.[14,110,111] The work we report here strongly suggests that lead's negative impact on protein function arises from Pb(II) binding in a three-coordinate mode and thus disrupting proper protein folding and DNA binding.

Conclusion

Critically, the results of the current study clearly indicate that the Pb(II) coordination sphere is significantly different from that of Zn(II) bound to the same peptides. Zinc binding to CP−CCCC is tetrahedral, with $Zn-S_4$ coordination; Zn(II) binding in CP−CCCH, CP−CCHC, and HIV−CCHC is also tetrahedral but with $Zn-S_3N$ coordination.[37,38,72,112,113] By contrast, Pb(II) in both CP−CCCC and CP−CCCH is three-coordinate, $Pb-S_3$. Because tetrahedral zinc coordination is essential for proper folding of these peptides,[13,28] these results provide a simple explanation for the observation that Pb(II) does not induce proper folding of the peptides, even when it binds *more tightly* than zinc.[13]

Structural zinc-binding domains are commonly found in transcription factors and proteins involved in gene expression.[114,115] In these proteins, the zinc-binding domain is the part of the protein that directly binds to DNA; improper folding of these domains will reduce or prevent protein−DNA binding. The studies reported here provide the first detailed, molecular insights into how lead binding to these proteins could directly account for some of the severe developmental problems known to result from lead poisoning.

Acknowledgment. We acknowledge J. T. Rijssenbeek and H. B. Gray for helpful discussions. We thank the National Institutes of Health (GM-58183 to H.A.G., GM-38047 to J.P.H., and GM-46502 to G.P.) and the National Science Foundation (CHE-9875341 and CHE-9810378 to H.A.G.) for support of this research. Synchrotron measurements were made at SSRL, which is supported by the NIH Research Resource program and the U.S. DOE. H.A.G. acknowledges additional support from the Burroughs Wellcome Fund, the Camille and Henry Dreyfus Foundation, and the Sloan Foundation. J.S.M. acknowledges support from an NIH Institutional NRSA Training Grant in Molecular Biophysics (GM-08382) and from the Institute for Environmental Catalysis at Northwestern University, funded by the NSF and U.S. DOE (NSF CHE-9810378). G.P. also acknowledges support from the NSF and U.S. DOE via the Columbia University Environmental Molecular Sciences Institute (NSF CHE-9810367).

Supporting Information Available: Crystal data and structure refinement for **2** (Table S1), comparison of key XAS and crystal structure distances for **2** (Table S2), XANES and EXAFS spectra for all Pb−peptide complexes measured (Figures S1, S2), fits for the CP−CCXX EXAFS data (Figure S3), UV−vis absorption spectra of apo peptides (Figure S4), representative metal binding titration data and fits (Figures S5, S6). This material is available free of charge via the Internet at http://pubs.acs.org. Crystal structure data for $[AsPh_4]_4[Pb(i\text{-mnt})_2]_2$ have been deposited with the Cambridge Crystallographic Data Centre (deposition number CCDC 258284).

JA0424530

(107) Busenlehner, L. S.; Cosper, N. J.; Scott, R. A.; Rosen, B. P.; Wong, M. D.; Giedroc, D. P. *Biochemistry* **2001**, *40*, 4426−4436.
(108) Busenlehner, L. S.; Weng, T.-C.; Penner-Hahn, J. E.; Giedroc, D. P. *J. Mol. Biol.* **2002**, *319*, 685−701.
(109) Apuy, J. L.; Busenlehner, L. S.; Russell, D. H.; Giedroc, D. P. *Biochemistry* **2004**, *43*, 3824−3834.
(110) Rous, B. W. Spectroscopic analysis of the interaction of lead with the glucocorticoid receptor DNA-binding domain: A possible mechanism of lead toxicity. Ph.D. Thesis, Northwestern University, Evanston, IL, 2004.
(111) Payne, J. C. Spectroscopic analysis of the interactions between lead and structural zinc-binding domains. Ph.D. Thesis, Northwestern University, Evanston, IL, 2002.
(112) Worthington, M. T.; Amann, B. T.; Nathans, D.; Berg, J. M. *Proc. Natl. Acad. Sci. U.S.A.* **1996**, *93*, 13754−13759.
(113) Amann, B. T.; Worthington, M. T.; Berg, J. M. *Biochemistry* **2003**, *42*, 217−221.
(114) Berg, J. M. *Acc. Chem. Res.* **1995**, *28*, 14−19.
(115) Berg, J. M.; Shi, Y. *Science* **1996**, *271*, 1081−1085.